

## AN EXOPLANET DETECTION ALGORITHM FOR FIELD-ROTATED CORONAGRAPHIC IMAGES, AND PRELIMINARY RESULTS FOR SPHERE.

I. Smith<sup>1</sup>, A. Ferrari<sup>1</sup>, M. Carillet<sup>1</sup>, A. Boccaletti<sup>2</sup>, T. Fusco<sup>3</sup>, K. Dohlen<sup>4</sup>, D. Mouillet<sup>5</sup> and M. Langlois<sup>4</sup>

**Abstract.** The VLT Planet Finder SPHERE (Spectro-Polarimetric High-contrast Exoplanet REsearch), that will include extreme adaptative optics (AO) and high-contrast coronagraphy, is under development. While observing exoplanets with one of the facilities of SPHERE –IRDIS (Infra-Red Dual-beam Imaging and Spectroscopy) in stabilized pupil mode– the field of interest rotates in the focal plane with respect to optical aberrations that arise from post-AO residuals and instrumental aberrations. We propose a detection-estimation algorithm, based on a likelihood approach, where we use this rotation effect as the main discriminating criterium between the planet and the speckles. We also propose an idea to extend the algorithm in order to take into account the Double Band Imaging facility given by IRDIS. The performance of the algorithm is evaluated by numerical simulations based on the code developed within the SPHERE consortium.

### 1 Detection-Estimation algorithm

The proposed algorithm tries to discriminate the planet from the background by the *detection of its motion*. This technique has already been proposed (Marois et al. 2006; Mugnier et al. 2007) but the present study does not focus on the same issues: previous work tries to suppress and stabilize the background using differential processing –but without making any estimation, whereas the solution presented herein tries to estimate the intensity and the position of a planet –but assuming that the background is perfectly static.

#### 1.1 Statistical model

In mathematical words, we use a simple data model: at time exposure  $k$  ( $k = 1 \dots N$ ), the vector  $x_k$  which consists in the  $M$  concatenated pixels of the camera, is expressed as

$$x_k = d + \alpha p_k(r) + \epsilon_k \quad (1.1)$$

where  $d$  is a *stationnary deterministic unknown* vector which represents the instrumental response (coronagraph, static speckles, ...),  $\alpha$  is the *unknown intensity* of a possible planet,  $r$  its *unknown position* on the first image,  $p_k$  its *known instrumental response* on the image  $k$ , and  $\epsilon_k$  a *noise vector* assumed Gaussian, independent from an image to another and with  $\epsilon_k \sim N(0, \sigma^2 I_M)$ , where  $\sigma$  is unknown.

The goal is to derive a detection algorithm ( $H_0: \alpha = 0$  vs  $H_1: \alpha > 0$ ) and give an estimation of  $\alpha$  and  $r$  for the detected planets.

---

<sup>1</sup> LUAN, Université de Nice Sophia-Antipolis

<sup>2</sup> LESIA, Observatoire de Paris Meudon

<sup>3</sup> ONERA

<sup>4</sup> LAM, OAMP, Université de Provence

<sup>5</sup> LATT, Observatoire Midi-Pyrénées

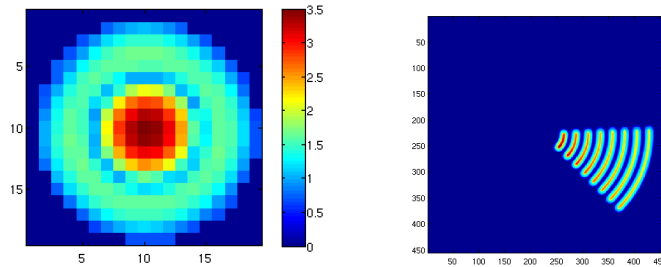


**Fig. 1.** Left:  $0''.32 \times 0''.32$  map of the PSF off-axis  $p$  (at the power of 0.2), from CAOS-SPHERE simulation (see text). Right: Field rotation simulation: time integration ( $\sum_{k=1}^N p_k(r)$ ) for 8 different initial positions  $r$  (at the power of 0.2).

### 1.2 Pre-estimation of the planet profile

Field rotation –a circular but not uniform rotation of the field– is a deterministic effect (Avila & Wirenstrand 2005), that only depends on the celestial coordinates of the star (declination  $\delta$  and hour angle HA), the starting time of observation  $t$  and the position  $O$  of the field rotation axis on the image. Then, we assume that the instantaneous planet profile  $p$  remains the same during the observation, and that we can estimate it, for example as the core of an Airy pattern, or the analytical expression of the response of the Lyot coronagraph (Ferrari 2007). And finally we get  $p_k$  as a continuous time integration of  $p$  submitted to field rotation (see Fig.1).

### 1.3 Maximum Likelihood approach: parameters estimation and detection

First we define the vector  $\theta = (d, \alpha)$  and the matrix  $M_k = (I|p_k)$  of size  $M \times (M + 1)^1$ , so that the model is linear in  $\theta$ :

$$x_k = M_k \theta + \epsilon_k \quad k = 1, \dots, N \quad (\text{or } X = M(r)\theta + \epsilon \text{ concatenating the } x_k \text{ into a } MN \times 1 \text{ vector}) \quad (1.2)$$

Then the maximization of the likelihood  $L(\theta, r, \sigma) = P(\{x_k\}_k; \theta, r, \sigma)$  is easily computed with respect to  $\theta$ , and we can note that its argmaximum is a function of  $r$  and not  $\sigma$ :

$$\hat{\theta}_r(r) = \left( \sum_{k=1}^N M_k^t(r) M_k(r) \right)^{-1} \sum_{k=1}^N M_k^t(r) x_k \quad \text{and in particular} \quad \hat{\alpha}_r(r) = \frac{N \sum_k p_k^t(r) x_k - \sum_k p_k^t(r) \sum_k x_k}{N \sum_k \|p_k(r)\|^2 - \|\sum_k p_k(r)\|^2}. \quad (1.3)$$

The model being linear with respect to  $\theta$ ,  $\hat{\theta}_r(r)$  is unbiased and statistically efficient<sup>2</sup> for the true initial position, so that if  $r$  was known we could not find a better estimator of  $\alpha$  within this model. In particular

$$\text{var}(\hat{\alpha}_r(r)) = \frac{N\sigma^2}{N \sum_k \|p_k(r)\|^2 - \|\sum_k p_k(r)\|^2}. \quad (1.4)$$

Then the detection is achieved thresholding  $\hat{\alpha}_r(n)$  for all  $n = 1, \dots, M$ . The threshold can be fixed in order to obtain the required probability of false alarm, after having estimated  $\sigma^2$  through

$$\hat{\sigma}^2_{\text{unbiased ML}} = \sum_{k=1}^N \frac{\|x_k - \hat{d}\|_{M'}^2}{M'(N-1) - 1} \quad (1.5)$$

where we only take into account the piece of the image where no planet is likely to contribute<sup>3</sup>. Then, on the areas where the threshold is reached, we could estimate  $r$  by  $\hat{r}_{ML} = \text{argmax}_r L(\hat{\theta}_r(r), r)$ , so that  $\hat{\alpha}_{ML} = \hat{\alpha}_r(\hat{r}_{ML})$ . But by simplicity, we began by the simple estimation  $\hat{r} = \text{argmax}_r \hat{\alpha}_r(r)$  followed by  $\hat{\alpha} = \hat{\alpha}_r(\hat{r})$ . And finally we

<sup>1</sup>where  $I$  is the identity matrix and  $p_k$  is the last column of  $M_k$

<sup>2</sup>Efficient: its variance reaches the Rao-Cramer bound.

<sup>3</sup>The true  $ML$  estimator of  $\sigma^2$  requires  $r$  to be estimated, so we should estimate  $r$  before the detection is performed, which would rise some other difficulties.

can get an estimation of  $\text{var}(\hat{\alpha})$  from the previous estimators.

The model proposed is easily extended to take into account  $N'$  calibration images  $y_k = d + \epsilon_k$  assuming that the noise variance and the static background  $d$  are identical between the two sets of images. The calibration images could be either some other star images or the rescaled simultaneous images of the field in the second band, if the planet was assumed to have a deep enough absorption band.

## 2 Simulations of the VLT instrument SPHERE

The data are obtained using the Software Package SPHERE v2.1 (Boccaletti et al. 2007), developed within the CAOS problem-solving environment (Carillet et al. 2004) and assuming the standard IRDIS simulation parameters (Langlois et al. 2007). We took 300 atmospheric realizations to model one long exposure and considered H2 filter data obtained with the apodized Lyot coronagraph. We apply field rotation on the obtained images choosing the stabilized pupil mode, and introduce the camera noises on our set of  $N=450$  resulting images. The main simulation parameters are reported in the table hereafter.

### Main parameters

<b>Star and exoplanet system</b>	
intensity ratio	1.6 $10^{-6}$
separation angles	0.2, 0.5, 1 and 2 arcsec
star and planet types (Allard et al. 2001)	M0 at 10 pc, planet at 400K
declination, init. hour angle	0 deg , -2 hr
<b>Atmosphere+VLT</b>	
seeing (at 500 nm)	0.85 arcsec
wave-front outer-scale $\mathcal{L}_0$	25 m
jitter	3 mas
<b>SAXO system</b>	
guide star	mV = 8
sensor type	Shack-Hartmann (40×40)
<b>Near-IR coronagraph</b>	
wavelength band and resolution	$\lambda = 1.59 \mu\text{m}$ and R = 30
coronagraph type	apodized Lyot
mask and Lyot stop diameters	$4\lambda/D$ and $D$
chromatic upstream and downstream errors	0 nm and 10 nm
offset pointing	0.5 mas
<b>Aberrations</b>	
instr., AO calib., Fresnel prop.	34.5 nm, 7.4 nm, 4.7 nm
beam shift, defocus	8 nm, 4 nm
pupil shear, pupil rotation	0.002 D, 0 deg
<b>IRDIS imaging device</b>	
RON, flat-field noise	10 $e^-$ rms, $10^{-3}$ rms
sampling rate	Shannon at 0.95 $\mu\text{m}$
mean planet signal on the detector	19 electrons/s
time exposure	16 s
total integration	2 hr
field rotation velocity (pupil stabilized mode)	$v_{start}$ : 0.004 deg/s ; $v_{end}$ : 0.009 deg/s
Global (VLT + SPHERE) transmission	0.09

## 3 Results

While we cannot see any hint about the position of the planets on the sum of the derotated images, the planets located at  $0''.2$ ,  $0''.5$ ,  $1''$  and  $2''$  and  $1.6 \cdot 10^{-6}$  times less bright than the central star, appear well here (see Fig. 3, shown in a log view).

With the simple estimation  $\hat{r} = \text{argmax}_r \hat{\alpha}(r)$  on the thresholded map, the estimation of  $r$  is *within one pixel of the true position* for the four planets. Then we get a first idea of the accuracy of the estimation of  $\alpha$  by estimating the number of electrons due to the source on a single exposure by  $\hat{N}_\gamma = \hat{\alpha} \times \sum_{i=1}^M p_k(i)$  (for any  $k$ ) with  $\hat{\alpha} = \hat{\alpha}_r(\hat{r})$ . Then,  $\hat{N}_\gamma$  is *within 10% of the true value* for the four planets.

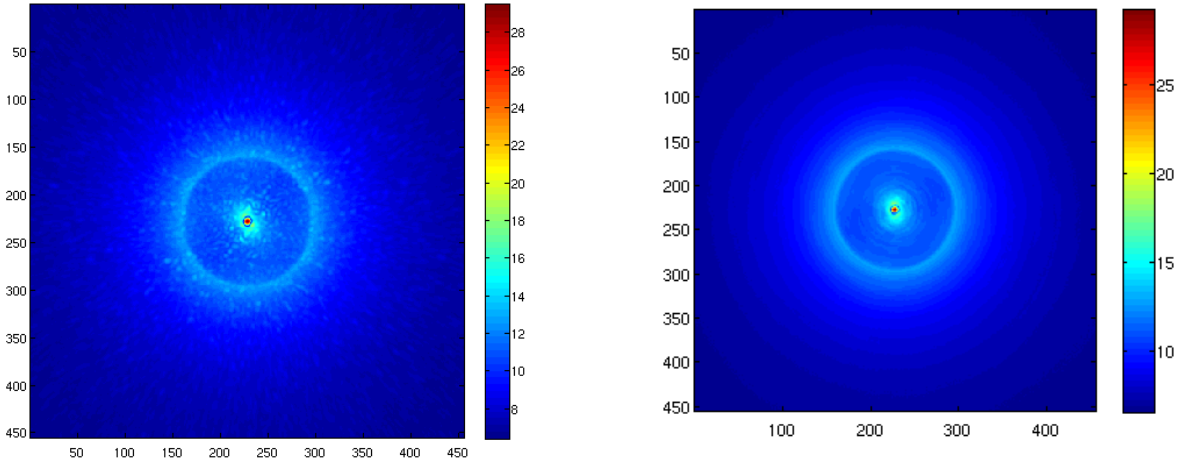


**Fig. 2.** Left: Sum of the 450 exposures  $\sum_{k=1}^{450} x_k$  (at the power of 0.2). Right: Sum of the exposures, after derotation (the planets are superimposed).

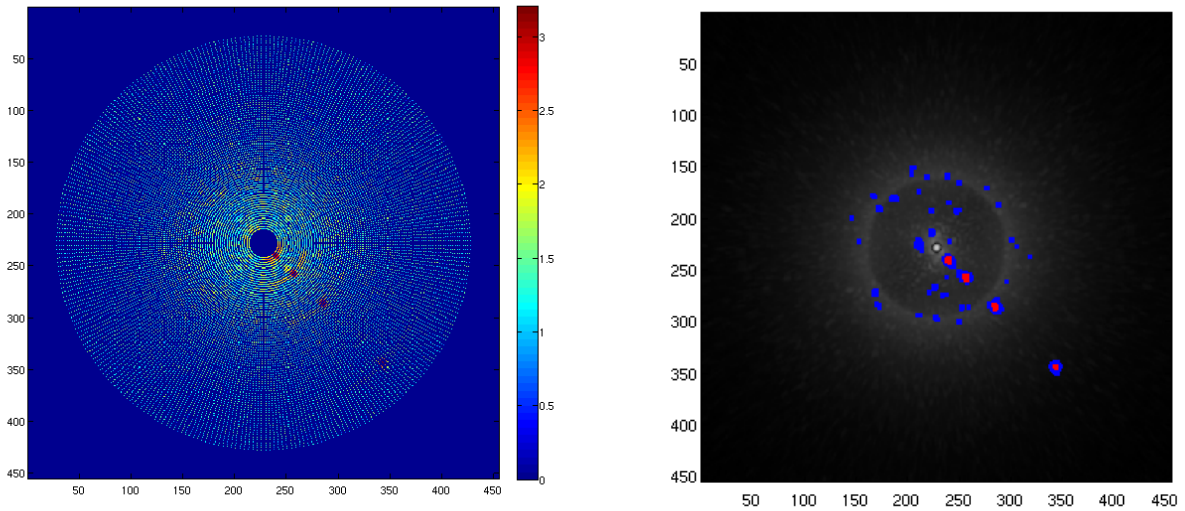


**Fig. 3.** Left: Estimation  $\hat{\alpha}_r(n)$  for all possible initial positions  $n$  (at the power of 0.2). Right:  $\hat{\alpha}_r(n)$  thresholded (and dilatated for clarity), and superimposed on the data in a log view.

## References

- Allard, F. et al. 2001, ApJ, 556, 357  
 Avila, G., & Wirenstrand, K. 2005, VLT-TRE-ESO-11000-3526  
 Boccaletti, A. et al. 2007, Simulation tool manual for Software Package SPHERE v2.1, VLT-MAN-SPH-14690-0230  
 Carillet, M. et al. 2004, SPIE Proc., 5490, 637  
 Ferrari, A. 2007, ApJ, 657, 1201  
 Langlois, M. et al. 2007, IRDIS simulation and performance analysis report, VLT-TRE-SPH-14690-0195  
 Marois, C. et al. 2006 ApJ, 641, 556  
 Mugnier, L. et al. 2007, Multi-Channel planet detection algorithm for angular differential imaging, in Opt. Soc. of A.